Effect of temperature on the structure and dynamic properties of metal sulphide nanostructures via molecular dynamics simulation

M A Mehlape, **T G Mametja, T E Letsoalo and P E Ngoepe**
Materials Modelling Centre, School of Physical and Mineral Sciences, University of Limpopo, South Africa, Private Bag, X1106, SOVENGA, 0727

Email:mofuti.mehlape@ul.ac.za

Abstract. Metal sulphide nanostructures via molecular dynamics (MD) simulations at different temperatures are presented and discussed in order to understand their structure and dynamic properties. Nanostructured metal sulphides have attracted the attention of researchers in the fields of materials science, physics and chemistry. They have enhanced structure and dynamic properties due to their large surface-to-volume ratio; hence making them desirable to a wide range of industries. They are promising materials for catalysis, batteries and photovoltaic, however the understanding on the structure and dynamic conditions of large-scale nanostructures are still to be explored more. Computational modelling technique, MD was performed to provide atomic or molecular level insights of the structure and dynamic properties of nanostructured metal sulphides. The effect of temperature on different sizes of nanostructures are analysed in a form of structure and dynamic properties; namely radial distribution functions, potential energy and diffusion coefficient. The results showed that temperature associated with the melting transition and stability increased with an increase in the nanostructure size.

1. Introduction

Nanoscience and nanotechnology collectively represent one of the fastest growing interdisciplinary scientific areas, spanning interests from physics, through chemistry and geoscience, to biology [1]. Nanostructures have been identified worldwide as the key to unlocking a new generation of devices with revolutionary properties and functionalities [2]. Nanostructures have many interesting properties (for example structural and dynamic properties), as they bridge the gap between bulk materials and atomic or molecular structures [3]. Nanostructures offer the advantages of high surface-to-volume ratios, favourable transport properties [4]. Herein, we report the effect of temperature on the structure and dynamic properties of metal sulphide, FeS_2 pyrite nanostructures. Pyrite, also known as Fool's Gold, is a very attractive next-generation photovoltaic (PV) material that is abundant in nature and nontoxic [5]. Various FeS_2 pyrite nanostructures such as nanostructures [6], nanocrystals [7], nanotubes [8] and nanowires [9] to name but a few, have been studied experimentally. However, experimental difficulties in studying nanostructures arise from their small size, which limits the use of traditional techniques for measuring other properties and conditions (such as physical, structural and dynamic properties, pressure and temperature) [10]. Hence, computational simulation is used to access those conditions that are sometimes difficult to obtain experimentally and simulation is also useful for planning experiments that require complicated setups [11]. Computational simulation technique, molecular dynamics (MD) is used to investigate the effect of temperature on the structure and dynamic properties of FeS_2 nanostructures.

1.1. Pyrite, FeS$_2$ structure

Cubic pyrite, FeS$_2$ belongs to the space group Pa3 [12]. FeS$_2$ has a NaCl-type cubic structure with the $(S_2)^{-2}$ groups situated at the cube centre and midpoints of the cube edges, and the low-spin Fe^{2+} atoms located at the corners and face centres [13]. Cubic FeS$_2$ structure together with the nanostructure are shown in Figure 1.
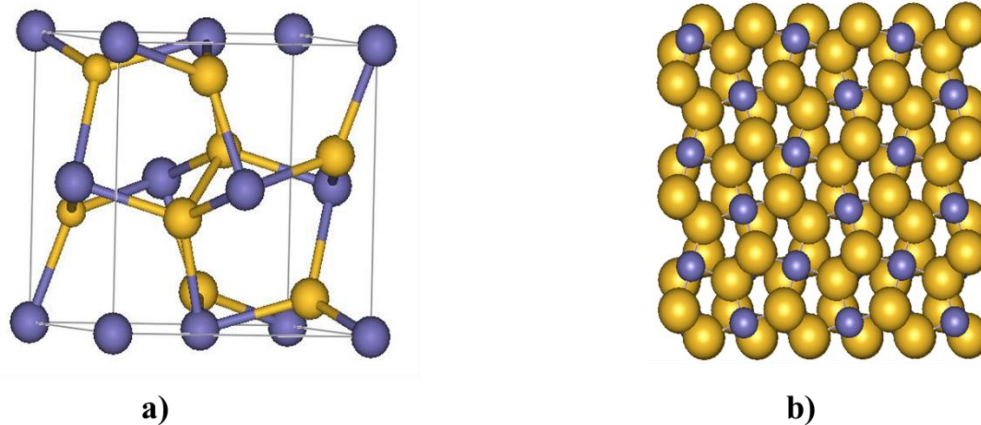
Figure 1: Snapshots of a) cubic bulk structure of pyrite, FeS$_2$, and b) Initial FeS$_2$ nanostructure, where purple atoms represent iron (Fe) and yellow atoms represent sulphur (S).

2. Computational Details

2.1. Creation of nanostructures and methodology

Initial configuration of FeS$_2$ nanostructures was constructed using METADISE code [14], which uses Wulff constructions [15] to predict the morphology. This approach follows the theory of Gibbs to generate the lowest total surface energy morphology from facets that may each have different surface energies. The stable {100} surface [16] was used to create its cubic nanostructures. MD simulations of nanostructures were performed with DLPOLY_2.20 code [17]. The MD simulation of the nanostructures were carried out in an ensemble approximating the canonical with constant number of atoms *N* and volume *V*. Temperature is controlled by a Nose-Hoover thermostat [18], in order to avoid steady energy drifts caused by the accumulation of numerical errors during MD simulations [19]. The equations of motion were integrated using the Verlet Leapfrog algorithm [20] with a time step of 1 fs. The constant temperature and volume simulations were performed over the temperature range of 300 K to 2000 K with 100 K increments at zero pressure for the nanostructures of between 1 nm and 4.5 nm in diameter. The sizes of the nanostructures of FeS$_2$ used in this study, and the corresponding number of FeS$_2$ units are given in Table 1. MD simulations were performed under non-periodic boundary conditions to make sure that the results are not affected by boundary conditions.

Table 1: Size of nanostructures (in diameter) and the corresponding number of FeS$_2$ units used for nanostructures.

Particle Dimension (nm)	Number of Atoms
1.0	96
1.5	324
2.9	1997
3.4	3295
4.5	7369

2.2. Representation of interatomic potentials

The Born ionic model [21] was used and parameters were derived for short range interactions represented by the Buckingham potential, harmonic function and three body terms:

2.2.1. Buckingham Potential

In the Buckingham potential, the repulsive term is replaced by an exponential term and potential takes the form

$$U(r_{ij}) = A_{ij} * exp^{-r_{ij}/\rho_{ij}} - \frac{C_{ij}}{r_{ij}} \qquad (1)$$

where A_{ij} and ρ_{ij} are parameters that represent the ion size and hardness, respectively, while C_{ij} describe the attractive interaction and r_{ij} is the distance between ion i and ion j. The first term is known as the Born-Mayer potential and the attraction term (second term) was later added to form the Buckingham potential. Very often, for the cation-anion interactions, the attractive term is ignored due to the very small contribution of this term to the short-range potential, or, alternatively, the interaction is subsumed into the A and ρ parameters.

2.2.2. Harmonic Potential

The interaction between the sulphur atoms of the S-S pair were described by a simple bond harmonic function:

$$U(r_{ij}) = \frac{1}{2} k_{ij}(r_{ij} - r_0)^2 \qquad (2)$$

where k_{ij} is the bond force constant, r_{ij} the interionic separation and r_0 the separation at equilibrium.

2.2.3. Three-Body Potential

A further component of the interactions of covalent species is the bond-bending term, which is added to take into account the energy penalty for deviations from the equilibrium value. Hence, this potential describes the directionality of the bonds and has a simple harmonic form:

$$U(\theta_{ijk}) = \frac{1}{2} k_{ijk}(\theta_{ijk} - \theta_0)^2 \qquad (3)$$

where k_{ijk} is the three-body force constant, θ_0 is equilibrium angle and θ_{ijk} is the angle between two interatomic vectors i - j and i - k. The potential parameters for the nanostructures of FeS$_2$ was previously successfully used for the investigation of bulk and surfaces of FeS$_2$ [16, 22].

## 3. Results and Discussions

3.1. Dynamic properties

Thermodynamically, the melting of bulk crystalline solids is characterized by a sudden increase in the free energy [23]. The curves of potential energy versus temperature for FeS$_2$ nanostructures were obtained. Figure 2 shows the potential energy variation with temperature for nanostructures with different number of atoms, i.e., 96, 324, 1997, 3295 and 7369 atoms, which corresponds to 1 nm, 1.5 nm, 2.9 nm, 3.4 nm and 4.5 nm in diameter, respectively. The phase transition from solid to liquid phase can be identified by a jump in the energy curve. The melting point of the FeS$_2$ nanostructures can be estimated from the change in slope of the temperature dependence of the energy. The variation of potential energy per atom of the system, with temperature for different nanostructure sizes is shown in Figure 2. The observation is that there is an increase in potential energy with temperature for all sizes. However the sudden steep increase in the rate of change of potential energy at a particular temperature, which is associated with the melting transition, is more apparent in the case of a nanostructure of 4.5 nm. This implies that as the size of the nanostructure increase, the temperature associated with melting transition is more apparent.
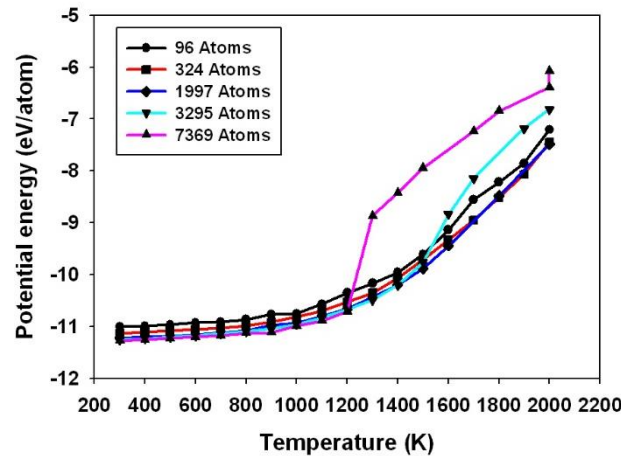
Figure 2: The potential energy per atom as a function of temperature for nanostructures with different number of atoms. Number of atoms corresponds to the diameters depicted on Table 1.

3.2. Structural properties

Radial distribution functions (RDFs) for FeS_2 nanostructures of 324 and 7369 atoms are shown in Figure 3 for Fe–Fe, Fe–S and S–S pairs at temperatures between 300 and 1500 K. RDFs describe the local coordination around a specific atom and represent the internal structure of a material [24]. The RDFs change from well-ordered to molten configuration for increasing temperature. The well-ordered configuration is characterised by a profile which manifests a greater number of narrower peaks with increasing radius. The molten configuration is characterised by a profile with both fewer and broader peaks. It can be observed that the RDFs show structural changes at different temperatures for different sizes of nanostructures. The nanostructure with 324 atoms, in Figure 3(a), has a crystalline and well-ordered structure, as observed by many peaks of the RDFs, from 300 to 500 K. The height of the peaks is also reduced as the temperature increases. The significant peak height reduction for the Fe–Fe, Fe–S and S–S pairs is observed at 1000 K; whereby the peaks become smoother, indicative of a liquid phase of the nanostructure with 324 atoms. The nanostructures with 7369 atoms at the temperatures leading to the melting are shown in Figure 3(b). It can be deduced from the many peaks of the RDFs that from 300 to 1000 K, the nanostructures has a crystalline and well-ordered structure. At 1000 K the peaks start to broaden and the height has decreased substantially as compared to those at lower temperatures; however at 1500 K the peaks are broadened and smoother, indicative of the liquid phase of the nanostructure with 7369 atoms.
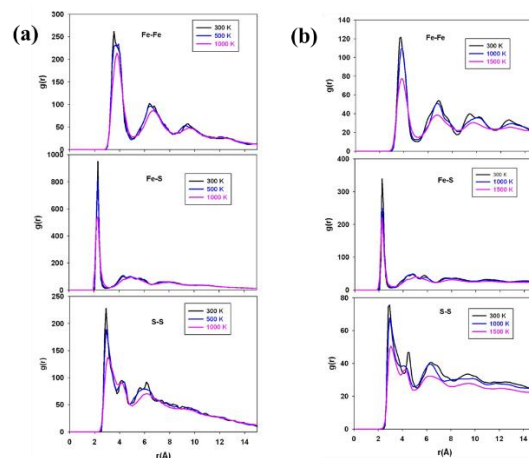
Figure 3: The radial distribution functions (RDFs) of FeS_2 nanostructures at various temperatures with different number of atoms. (a) 324 atoms and (b) 7369 atoms.
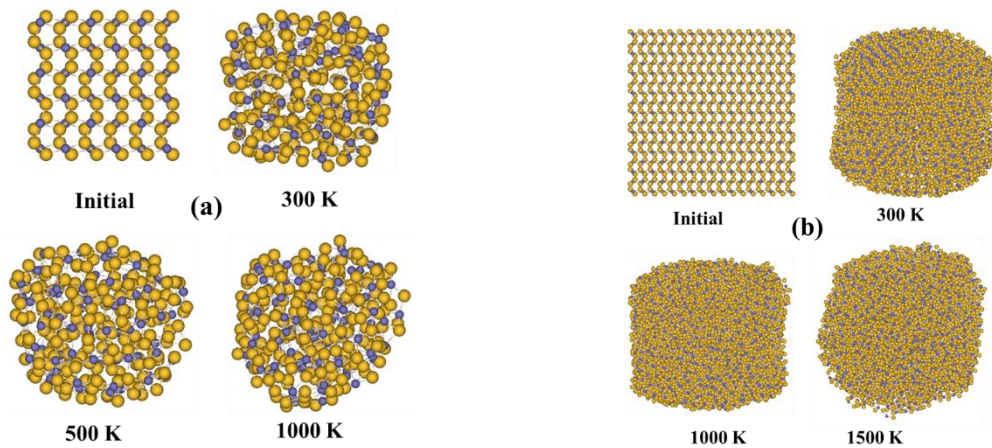
Figure 4: Structural changes of FeS$_2$ nanostructures with a) 324 atoms and b) 7369 atoms before and after MD simulation at different temperatures.

Figure 4 show the initial configuration structures and the structural changes of FeS$_2$ nanostructures (with 324 and 7369 atoms) at elevated temperatures. It can be seen that the nanostructures retain their cubic shapes more below the transition temperature as the particle size increases. For a nanostructure with 324 atoms the cubic structure is maintained at the temperature of 300 K, however at the elevated temperatures (from 500 K), the atomic arrangement disappear. In the case of a nanostructure with 7369 atoms the cubic shape is maintained up to the temperature of 1000 K, and disordering is observed at a higher temperature of 1500 K. This implies that the structural stability of the nanostructure is retain at higher temperature as the particle size increases.

4. Conclusion

Molecular dynamics simulations were performed with the aim of investigating the dynamic and structural properties of pyrite FeS$_2$ nanostructures. It was observed that the temperature of melting transition increased with an increase in particle size. The melting of nanostructures was observed through the variation of energy as a function of temperature, whereby there is a sudden change of slope at a certain temperature, indicative of phase transition. At low temperatures the RDFs have many and sharp peaks, however, at higher temperatures the RDFs curve are relatively smooth and does not exhibit any defined peaks, indicative of structural change from solid to liquid phase. The height of the peaks are also reduced as the temperature increases. The structural snapshots suggest that the nanostructure with less number of atoms maintain their cubic shape up to 500 K and for the nanostructures with large number of atoms maintain their cubic form up to 1000 K. This implies that the stability of the nanostructure increase as the particle size increases. We further observed that the change in energy gradient associated with the melting transition occurred at almost similar temperatures associated with the stretching and broadening of the RDFs. Molecular dynamic simulations of FeS$_2$ nanostructures provided in this study will give more understanding in the prediction of their structural and dynamic properties for developing new applications, especially in the next-generation of photovoltaic. Furthermore, the properties presented in this study could form as a basis for future studies.

References
[1] Spagnoli D and Gale J G 2012 *Nanoscale* **4** 1051.
[2] Akbarzadeh H, Abroshan H and Parsafar G A, 2010 *Solid State Commun.* **150**, 254.
[3] Heikkila E, Martinez-Seara A A, Hakkinem H, Vattulainen l and Akola J 2012 *J. Phys. Chem.* **166**, 9805.
[4] Rui X, Tan H and Yan Q 2014 *Nanoscale* **6** 9889.

[5] Bi Y, Exstrom C L, Darveau S A and Huang I 2012 *Nano Lett.* **11**, 4953.

[6] Chin P P, Ding J, Yi J B and Liu B H 2005 *J. Alloys. Compd.* **390** 255.

[7] Trinh T K, Pham V T H, Truong N T N, Kim C D and Park C 2017 *J. Cryst. Growth*. **461** 53.

[8] Macpherson H and Stoldt C R 2012 *ACS Nano* **6**, 8940.

[9] Caban-Acevedo M, Faber M S., Tan Y, Hamers R J and Jin S 2012 *Nano Lett.* **12** 1977.

[10] Suh Y J, Prikhodko S V and Friedlander S K *Microsc. Microanal.* 2002 **8** 497.

[11] Rodrigues A M, Rino J P, Pizani P S and Zanotto E D 2016 *J. Phys. D: Appl. Phys.* **49** 1.

[12] Liu S, Li Y, Yang J, Tian H, Zhu B and Shi Y 2014 *Phys. Chem. Miner*. **41** 189.

[13] Huang S-Y, Sodano D, Leonard T, Luiso S and Fedkiw P S 2017 *J. Electrochem. Soc.* **164** F276.

[14] Watson G W, Kelsey E T, de Leeuw N H, Harris D J and Parker S C 1996 *J. Chem. Soc. Faraday Trans* **92** 433.

[15] Wulff G Z 1901 *Krystallogr. Minera.* **34** 449.

[16] Mehlape M A, Parker S C and Ngoepe P E 2015 in *Proceedings of the 60th Annual Conference of the South African Institute of Physics* edited by M. Chithambo and A. Venter, (SAIP2015, Richard's Bay, South Africa,) 67.

[17] Smith W and Forester T R 1996 *J. Mol. Graphics* **14** 136.

[18] Nosé S 1990 *J. Phys.:Condens. Matt*er **2** 115.

[19] Rühle V 2008 *Berendsen and Nose-Hoover thermostats* http://www2.mpipmainz.mpg.de/~andrienk/journal club/thermostats.pdf, (University of Mainz, Journal Club) Accessed 02 May 2019.

[20] Verlet L 1967 *Phys. Rev*. **159** 98.

[21] Born M and Huang K 1954 *Dynamical Theory of Crystal Lattices,* 1st ed. (University Press, Oxford).

[22] de Leeuw N H, Parker S C, Sithole H M and Ngoepe P E 2000 *J. Phys. Chem. B* **104** 7969.

[23] Adnan A and Sun C T 2008 *Nanotechnology* **19** 1.

[24] Okeke G, Antony S J, Hammond R B and Ahmed K 2017 *J. Nanopart. Res.* **19** 237.